ORIGINAL PAPER

A NOVEL SCHEME BASED ON COLLOCATION FINITE ELEMENT METHOD TO GENERALISED OSKOLKOV EQUATION

SEYDI BATTAL GAZI KARAKOC[1,*], SAMIR KUMAR BHOWMIK [2], DERYA YILDIRIM SUCU[1]

Manuscript received: 10.06.2021; Accepted paper: 17.10.2021; Published online: 30.12.2021.

Abstract. *This article is concerned with designing numerical schemes for the generalised Oskolkov equation using the quintic B-spline collocation finite element method. Applying the von-Neumann theory, it is shown that the proposed method is marginally unconditionally stable. It was obtained the theoretical bound of the error in the full discrete scheme for the first time in the literature. The accuracy and effectiveness of the method checked with three model problems, consisting of a single solitary wave, Gaussian initial condition and growth of an undular bore. The performance of the new method is demonstrated by calculating invariant* I *and error norms* L_2 *and* L_∞*. Results are displayed both numerically and graphically. Numerical experiments support the correctness and robustness of the method which can be further used for solving such problems.*

Keywords: *Generalised Oskolkov equation; shock wave; finite element method; collocation; quintic B-splines.*

1. INTRODUCTION

In recent years, nonlinear evolution equations have played a crucial role in describing complex phenomena that arise in different scientific subjects such as wave propagation, thermodynamics, soil consolidation, rock discontinuities and optical fibers [1]. The mentioned equations have become a widely studied subject in science and engineering due to their use in modeling natural phenomena. Therefore, the solutions obtained from these equations give a great idea about the physical behavior of the related problems. In the past few decades, a wide variety of analytical approaches, such as the modified simple equation method, have been developed and sensitive solutions have been found and significant progress has been made. Examining the dynamics of the nonlinear evolution equations, it can be discovered that several nonlinear systems may provide some solutions for a given set of parameter values and various initial conditions [2]. It should be noted, however, exact solutions of these equations are mostly not procurable, in particular when the nonlinear terms are involved. Since only a finite number of classes of these partial differential equations are solved analytically, numerical solutions are highly functional for studying physical phenomena.

Many scientists have created a walking wave solution by applying various methods

[1] Nevsehir Haci Bektas Veli University, Faculty of Science and Art, Department of Mathematics, 50300 Nevsehir, Turkey. E-mail: sbgk44@gmail.com.
[2] University of Dhaka, Department of Mathematics, 1000 Dhaka, Bangladesh.
E-mail: bhowmiksk@gmail.com.
**Corresponding author: sbgk44@gmail.com.*

through nonlinear partial differential equations [3]. For instance, Well-established procedures such as extended Kudryashov method, New extended $(G'/G)-$expansion method, Darboux transform, Modified simple equation method (Msem), Trial solution method in extended literature, Jacobian elliptic function method, Inverse engineering method, Fokas method, Exp-function method, Multiple simplest equation method, Sin-cosine method etc. [4-14]. The exact solutions of the various types of Oskolkov equation have been studied by a number of different methods [15-17]. For the Oskolkov equation, with the help of the computer algebraic system Maple, the (G′/G) expansion method has been proposed to search for solutions of moving waves [18]. Mamunur discovered complete and clear solution of Oskolkov equation with the (Mse) method [19], Faruk, found abundant new solutions of equation by the tanh-coth method [20], Ak et al. [21] presented the shock wave solutions by applying the unified method and Bashar [3] compiled the adaptation of the exact nonlinear wave solutions for Oskolkov equations by applying the simple linear equation method.

In this article solutions of the generalised Oskolkov equation are presented by using collocation finite element method. The collocation approach mentioned is based on collocation of quintic B-splines over spatial finite elements. Since the spline functions are fragmented polynomials, they can be integrated and differentiated and most of the integral in numerical methods is zero. In this way, B-spline functions are applied to numerical methods to get the solution of partial differential equations. In addition, these methods based on spline functions to obtain numerical solutions of differential equations lead to band matrices that can be easily resolved with low cost calculations and some algorithms in the market. The one-dimensional Oskolkov equation can be defined as follows:

$$U_t - \lambda U_{xxt} - \alpha U_{xx} + UU_x = 0.$$

This equality is the pseudoparabolic equation and the one-dimensional analogue of the Oskolkov system indicates the dynamic behavior of the Kelvin - Voigt model of viscoelastic fluids. The parameter λ may be a negative value, but a negative value of λ does not distort the physical meaning of the Oskolkov equation. The parameters u and λ feature the viscous and elastic properties of the fluid, respectively [22].

In this study, the motions of shallow water waves, modeled by the generalised Oskolkov equation with the quintic B spline collocation finite element method has been examined. The plan of this paper is as follows: Some preliminary results of quintic B-spline and the stability analysis of the scheme are well studied in Section 2 and Section 3. Convergence of the full discrete scheme is examined in Section 4. In Section 5, some numerical model problems are presented. A conclusion is given in Section 6.

2. NUMERICAL APPLICATIONS OF THE SCHEME

In this section, the following generalised Oskolkov equation is examined

$$U_t + \gamma(U^p)_x + \sigma U_{xx} + \eta U_{xxt} = 0 \qquad (2.1)$$

which has need for the boundary conditions $U \to 0$ as $x \to \pm\infty$, where γ, σ and η are constants and x is the space coordinate and t symbolizes time differentiation.

First of all, the nodes are divided into N intervals equal to the problem domain

$a \le x \le b$ like that $a = x_0 < x_1 < ... < x_N = b$ with mesh spacing $h = \frac{b-a}{N}$. for $m = 1, 2, ..., N$. Boundary conditions have been taken into account from the following homogeneous conditions:

$$\begin{aligned} &U_N(a,t) = 0, \qquad U_N(b,t) = 0, \\ &(U_N)_x(a,t) = 0, \qquad (U_N)_x(b,t) = 0, \ t > 0 \end{aligned} \tag{2.2}$$

and the initial condition $U(x,0) = f(x), \ a \le x \le b.$

The quintic B-splines $\psi_m(x)$, $(m = -2(1)N+2)$, at the knots x_m with the required properties are described by Prenter [23]:

$$\psi_m(x) = \frac{1}{h^5}\begin{cases} (x-x_{m-3})^5, & [x_{m-3}, x_{m-2}] \\ (x-x_{m-3})^5 - 6(x-x_{m-2})^5, & [x_{m-2}, x_{m-1}] \\ (x-x_{m-3})^5 - 6(x-x_{m-2})^7 + 15(x-x_{m-1})^5, & [x_{m-1}, x_m] \\ (x-x_{m-3})^5 - 6(x-x_{m-2})^5 + 15(x-x_{m-1})^5 - 20(x-x_m)^5, & [x_m, x_{m+1}] \\ (x-x_{m-3})^5 - 6(x-x_{m-2})^5 + 15(x-x_{m-1})^5 - 20(x-x_m)^5 & \\ +15(x-x_{m+1})^5, & [x_{m+1}, x_{m+2}] \\ (x-x_{m-3})^5 - 6(x-x_{m-2})^5 + 15(x-x_{m-1})^5 - 20(x-x_m)^5 & \\ +15(x-x_{m+1})^5 - 6(x-x_{m+2})^5, & [x_{m+2}, x_{m+3}] \\ 0 & \textit{otherwise.} \end{cases} \tag{2.3}$$

Each quintic B-spline embeds six elements so that each element $[x_m, x_{m+1}]$ is covered by six spline functions. The spline functions $\psi_m(x)$ and its principal derivatives disappear outside the interval $[x_{m-3}, x_{m+3}]$. To solve the boundary value problem (2.1) using quintic B-splines as approximation functions by the collocation method, the following approximate solution $U_N(x,t)$ is expressed as

$$U_N(x,t) = \sum_{j=-2}^{N+2} \psi_j(x)\delta_j(t) \tag{2.4}$$

where $\delta_j(t)$ are time-dependent parameters specified from the collocation and boundary conditions. Substituing the quintic B-spline interpolation functions (2.3) into the trial function (2.4), four fundamental derivatives of $U(x,t)$ relating to at the knots are determined in terms of the time parameters δ_m by

$$\begin{aligned} &U_N(x_m,t) = U_m = \delta_{m-2} + 26\delta_{m-1} + 66\delta_m + 26\delta_{m+1} + \delta_{m+2}, \\ &U_m' = \tfrac{5}{h}(-\delta_{m-2} - 10\delta_{m-1} + 10\delta_{m+1} + \delta_{m+2}), \\ &U_m'' = \tfrac{20}{h^2}(\delta_{m-2} + 2\delta_{m-1} - 6\delta_m + 2\delta_{m+1} + \delta_{m+2}), \\ &U_m''' = \tfrac{60}{h^3}(-\delta_{m-2} + 2\delta_{m-1} - 2\delta_{m+1} + \delta_{m+2}), \\ &U_m^{iv} = \tfrac{120}{h^4}(\delta_{m-2} - 4\delta_{m-1} + 6\delta_m - 4\delta_{m+1} + \delta_{m+2}). \end{aligned} \tag{2.5}$$

Using the node values of U_m and its space derivatives given by Eqs. (2.5) in Eq. (2.1),

following combined the set of ordinary differential equations are obtained:

$$\begin{aligned}&(\dot{\delta}_{m-2}+26\dot{\delta}_{m-1}+66\dot{\delta}_m+26\dot{\delta}_{m+1}+\dot{\delta}_{m+2})+\tfrac{5\gamma Z_m}{h}(-\delta_{m-2}-10\delta_{m-1}+10\delta_{m+1}+\delta_{m+2})\\&+\frac{20\sigma}{h^2}\left(\delta_{m-2}+2\delta_{m-1}-6\delta_m+2\delta_{m+1}+\delta_{m+2}\right)+\frac{20\eta}{h^2}\left(\dot{\delta}_{m-2}+2\dot{\delta}_{m-1}-6\dot{\delta}_m+2\dot{\delta}_{m+1}+\dot{\delta}_{m+2}\right)=0,\end{aligned}\qquad (2.6)$$

where $Z_m = pU_m^{p-1} = p(\delta_{m-2}+26\delta_{m-1}+66\delta_m+26\delta_{m+1}+\delta_{m+2})^{p-1}$, and $\dot{}$ states derivative with respect to t. The term pU^{p-1} in non-linear term $pU^{p-1}U_x$, is received as Eq. (2.6) considering that the quantity pU^{p-1} is locally constant, with the linearization form presented by Rubin and Graves [24]. The equation given by (2.6) is decomposed by δ_i's and its time derivatives $\dot{\delta}_i$'s by the following Crank-Nicolson formula

$$\delta_i = \frac{\delta_i^{n+1}+\delta_i^n}{2}, \qquad (2.7)$$

and routine finite difference approach

$$\dot{\delta}_i = \frac{\delta_i^{n+1}-\delta_i^n}{\Delta t}. \qquad (2.8)$$

This approximation leads to the following recurrence relationship between two-time levels n and $n+1$ depending two unknown parameters δ_i^{n+1}, δ_i^n:

$$\begin{aligned}&\gamma_1\delta_{m-2}^{n+1}+\gamma_2\delta_{m-1}^{n+1}+\gamma_3\delta_m^{n+1}+\gamma_4\delta_{m+1}^{n+1}+\gamma_5\delta_{m+2}^{n+1}\\&=\gamma_5\delta_{m-2}^{n}+\gamma_4\delta_{m-1}^{n}+\gamma_3\delta_m^{n}+\gamma_2\delta_{m+1}^{n}+\gamma_1\delta_{m+2}^{n}\end{aligned}\qquad (2.9)$$

where

$$\begin{aligned}&\gamma_1=\left[1-EZ_m+K+M\right],\\&\gamma_2=\left[26-10EZ_m+2K+2M\right],\\&\gamma_3=\left[66-6K-6M\right],\\&\gamma_4=\left[26+10EZ_m+2K+2M\right],\\&\gamma_5=\left[1+EZ_m+K+M\right],\\&m=0,1,2,...,N,\ E=\frac{5\gamma}{2h}\Delta t,\ K=\frac{10\sigma}{h^2}\Delta t,\ M=\frac{20\eta}{h^2}\Delta t.\end{aligned}\qquad (2.10)$$

The system (2.9) consists of $(N+1)$ equations in $(N+5)$ unknown values $(\delta_{-2},\delta_{-1},\ldots,\delta_{N+1},\delta_{N+2})^T$. To get a unique solution to this system, four additional constraints are required. Boundary conditions are applied to eliminate the parameters δ_{-2},δ_{-1} and $\delta_{N+1},\delta_{N+2}$ from the system (2.9). In this case, this becomes a matrix equation for the $(N+1)$ unknowns $d^n=(\delta_0,\delta_1,\ldots,\delta_N)^T$ of the form

$$P\mathbf{d^{n+1}} = Q\mathbf{d^n}. \qquad (2.11)$$

The resulting system is solved with the Thomas algorithm and is implemented two inner iterations $\delta^{n*} = \delta^n + \frac{1}{2}(\delta^n - \delta^{n-1})$ at each time step to deal with the non-linearity caused by Z_m. Before the commencement of the solution process, the initial state vector d^0 must be determined from the initial condition and the following derivatives at the boundaries:

$$\begin{aligned} U_N(x,0) &= U(x_m,0); \qquad m = 0,1,2,...,N \\ (U_N)_x(a,0) &= 0, \qquad (U_N)_x(b,0) = 0, \\ (U_N)_{xx}(a,0) &= 0, \qquad (U_N)_{xx}(b,0) = 0. \end{aligned} \tag{2.12}$$

Thus, considering Eq. (2.12), a penta-diagonal system of equations are obtained and written in the following matrix form for the initial state vector d^0;

$$Wd^0 = R,$$

where

$$W = \begin{bmatrix} 54 & 60 & 6 & & & & & & \\ 25.25 & 67.50 & 26.25 & 1 & & & & & \\ 1 & 26 & 66 & 26 & 1 & & & & \\ & 1 & 26 & 66 & 26 & 1 & & & \\ & & & & \ddots & & & & \\ & & & 1 & 26 & 66 & 26 & 1 & \\ & & & & 1 & 26.25 & 67.50 & 25.25 & \\ & & & & & 6 & 60 & 54 & \end{bmatrix} \begin{bmatrix} \delta_0 \\ \delta_1 \\ \vdots \\ \vdots \\ \vdots \\ \vdots \\ \delta_{N-1} \\ \delta_N \end{bmatrix} = \begin{bmatrix} U(x_0,0) \\ U(x_1,0) \\ \vdots \\ \vdots \\ \vdots \\ \vdots \\ U(x_{N-1},0) \\ U(x_N,0) \end{bmatrix}$$

$d^0 = (\delta_0, \delta_1, \delta_2, ..., \delta_{N-2}, \delta_{N-1}, \delta_N)^T$ and $R = (U(x_0,0), U(x_1,0), ..., U(x_{N-1},0), U(x_N,0))^T$.

3. STABILITY OF THE SCHEME

For determining behaviour of the systems, stability is probably the first and most important problem to deal with it. Stability plays a significant role for studying on numerical approaches. Especially, for a discreating scheme, numerical stability is the most important concept [25]. In this section, the von-Neumann theory is employed to investigate the linear stability of the numerical scheme [26]. Growth factor ξ of a typical Fourier mode is identified as:

$$\delta_m^n = \xi^n e^{im\kappa h}, \ (i = \sqrt{-1}). \tag{3.1}$$

Substituting the Eq. (3.1) into the scheme (2.9), following equality is obtained:

$$\begin{aligned} &\xi^{n+1}(\eta_1 e^{i(m-2)\theta} + \eta_2 e^{i(m-1)\theta} + \eta_3 e^{i(m)\theta} + \eta_4 e^{i(m+1)\theta} + \eta_5 e^{i(m+2)\theta}) \\ &= \xi^n(\eta_5 e^{i(m-2)\theta} + \eta_4 e^{i(m-1)\theta} + \eta_3 e^{im\theta} + \eta_2 e^{i(m+1)\theta} + \eta_1 e^{i(m+2)\theta}) \end{aligned} \tag{3.2}$$

where κ is mode number, h is the element size, $\theta = \kappa h$. By implementing Euler's formula to the Eq.(3.2), the following growth factor is obtained

$$\xi = \frac{\mathrm{A} - iB}{A + iB}$$

where

$$A = (2\omega_1 + 2\omega_3 + 2\omega_4)\cos(2\theta) + (48\omega_1 + 4\omega_3 + 4\omega_4)\cos(\theta) + 66\omega_1 - 6\omega_3 - 6\omega_4,$$
$$B = 2\omega_2 \sin(2\theta) + 20\omega_2 \sin(\theta),$$

and

$$\omega_1 = 1, \quad \in \omega_2 = \frac{5\gamma}{2h} Z_m \Delta t, \quad \omega_3 = \frac{10}{h^2}\sigma\Delta t, \quad \omega_4 = \frac{20}{h^2}\eta\Delta t, \quad m = 0,1,...,N.$$

According to the Fourier stability analysis, for the given scheme to be stable, the condition $|\xi| < 1$ must be satisfied. Because of $|\xi| = 1$, is find that the linearized scheme is unconditionally stable.

4. CONVERGENCE OF THE FULL DISCRETE SCHEME

In this study generalised Oskolkov equation which is a non-linear PDE is integrated using collocation B-splines in space followed by a one step scheme for temporal approximation. It is to note that the performance of a numerical scheme depends on its error reduction and computational stability. Finite element schemes are very much popular for their priori and a posteriori estimates of convergence rates as well as discretization errors. Mostly theories depend on a functional analysis framework which is well developed and discussed in numerous books and articles. Here, the relevant concepts and key results without proof and cite sources of a more complete treatment are studied. To be specific, to a brief survey about the error estimates of the above-mentioned space time scheme without a formal proof is opted. One may consult [27-32] and many other well-known references for a detail. It is mentioned that are employed some constants $C_i \geq 0$, which are necessary not the same for all the cases.

Usually global polynomial interpolations are used to integrate the solutions of differential equations for simple computational domain and when unknown curves are considered to be smooth enough. However, most real life models are considered when the solutions are not sufficiently smooth to support such a scheme and the computational domain is not usually simple rather it is complex. For these types of cases finite element schemes play an important role and performs very well for such a modelled problem.

Polynomials are smooth which is very important in approximation theory. It helps to approximate and analyze solutions using polynomial basis functions. Let it have $r+1$ data values. Then there is exactly one polynomial of degree at most r passing through the data points and the error in the interpolating polynomial is proportional to a power of the distance between the data points [27-30]. As stated above is used a collocation Quintic B-splines in space. It is well known that collocation scheme gives super-convergence at collocation points and it does not require an extra inner product to evaluate as of the Galerkin inner product approach [33]. So this approach is simpler and efficient to compute solutions.

Here, $H^k(\Omega)$ is a space of k times differentiable functions and $\|.\|_r$ as standard $H^k(\Omega)$ norm. Let v_h be an approximation to a function $v(x) \in H^k(\Omega)$ in Ω. Here $\|.\|_0$ stands for $L_2(\Omega)$ norm. Let h be the distance between the grids and $\Omega = \cup_i \Omega_i$, where $\Omega_i = [x_i,\ x_{i+1}], x_{i+1} = x_i + h$. It was observed from [29-35] that

$$\|v(x) - v_h(x)\| \leq Ch^{r+1} \|v\|_{r+1} \text{ where } 1 \leq r < k,$$

and v_h stands for interpolation by piecewise-polynomials of degree r (considering $\Omega = \cup_i \Omega_i$). This error is preserved by the Galerkin finite element approximation as well [30, 32].

Let w_h be a B-spline of degree less or equal k that approximates $w \in H_r(\Omega)$ for any natural number $r > 0$, then it is evident [27, 32, 34, 35] that

$$\|w(x) - w_h(x)\| \leq Ch^{m+1} \|w\|_{m+1} \ where \ 1 \leq m < r.$$

Here Quintic B-splines have been used for space integration. Thus, from the above quotations it is confirmed that obtained a $O(h^6)$ accuracy for the spatial approximation in $L_2(\Omega)$ norm [32]. For time a forward difference scheme has been used which is accurate of $O(\Delta t)$ in $L_2([0\,T])$ norm for some $T > 0$ [30]. So for the space time discretization the error bound is of the form

$$\|u(x,t) - u_h(x,t)\| \leq C_1 h^8 + C_2 \Delta t,$$

for a suitable $C_1 \geq 0$ and $C_2 \geq 0$.

5. COMPUTER APPLICATIONS AND DISCUSSIONS

In this section, numerical solutions of the generalised Oskolkov equation are considered for three problems which are including the motion of shock wave, evolution of solitary waves with Gaussian and undular bore initial conditions. The error norms given below are utilized to demonstrate how good the numerical scheme guesses the position and amplitude of the solution as the simulation proceeds:

$$L_2 = \left\|U^{exact} - U_N\right\|_2 \cong \sqrt{h \sum_{J=0}^{N} \left|U_j^{exact} - \left(U_N\right)_j\right|^2},$$

and

$$L_\infty = \left\|U^{exact} - U_N\right\|_\infty \cong \max_j \left|U_j^{exact} - \left(U_N\right)_j\right|,\ j = 1, 2, ..., N.$$

The generalised Oskolkov equation (2.1) owns only one invariant by

$$I = \int_a^b U dx \cong h \sum_{j=1}^{N} U_j^N$$

which correspond to mass.

5.1. PROPAGATION OF SHOCK WAVE

The shock wave solution of the Eq. (2.1) with boundary conditions as $U \to 0$ as $x \to \pm\infty$ is denoted by

$$U(x,t) = [A + BD\left(\frac{\mu}{2} - \frac{a\mu}{a + \cosh\left[\mu\left(x - kt \right) - \sinh\left[\mu\left(x - kt \right) \right] \right]} \right)]^{2/p-1}, \qquad (5.1)$$

where

$$A = -\frac{1}{2}\frac{\sigma(p-1)\sqrt{\dfrac{\gamma\sigma\left(\sigma^2 - \dfrac{8\sigma^2\left(p+1 \right)}{\left(p+3 \right)^2} \right)\sqrt{2\eta\left(p+1 \right)}}{\gamma\left(p+3 \right)}}}{\gamma\left(p+3 \right)\left(\sigma^2 - \dfrac{8\sigma^2\left(p+1 \right)}{\left(p+3 \right)^2} \right)},$$

$$B = \frac{1}{\gamma\left(p+3 \right)\left(\sigma^2 - \dfrac{8\sigma^2\left(p+1 \right)}{\left(p+3 \right)^2} \right)},$$

$$D = \sigma\sqrt{2\eta\left(p+1 \right)}\sqrt{\frac{\gamma\sigma\left(\sigma^2 - \dfrac{8\sigma^2\left(p+1 \right)}{\left(p+3 \right)^2} \right)\sqrt{2\eta\left(p+1 \right)}}{\eta\left(p+3 \right)}},$$

$$\mu = \frac{\sqrt{8}}{4}\sqrt{\frac{p^2 - 2p + 1}{\eta\left(p+1 \right)}}, \qquad k = \frac{\sigma\sqrt{2\eta\left(p+1 \right)}}{\eta\left(p+3 \right)}$$

and a, k, μ, p are arbitrary constants. Initial condition is obtained as

$$U(x,0) = [A + BD\left(\frac{\mu}{2} - \frac{a\mu}{a + \cosh\left(\mu x \right) - \sinh\left(\mu x \right)} \right)]^{2/p-1}. \qquad (5.2)$$

The values of parameters are chosen as $\sigma = 0.1,\ \eta = 7,\ h = \Delta t = 0.1,\ \gamma = 0.5,\ 0.33,$ $p = 2, 3$ and $a = 0.3,\ 0.5$ through the interval $x \in \left[-50, 50 \right]$ for the computational work.

CASE 1.

For $p = 2,$ the parameters $\gamma = 0.5,\ \sigma = 0.1,\ \eta = 7,\ h = 0.1,\ a = 0.3$ and $\Delta t = 0.1$ are selected through the interval $-10 \le x \le 10.$ These parameters generate the amplitude $A = -0.096.$ The numerical simulations are performed to time $t = 5$ to calculate error norms L_2, L_∞ and the invariant $I.$ The values of the invariant and error norms provided by the suggested method are tabulated in Table (5.1). This table proves that the invariants remain

almost constant over time. Also, it have seen that the magnitude of the L_2 and L_∞ error norms is adequately small with increasing time and velocity, as expected. The behaviour of shock wave is plotted in Fig. (5.1). It is to notice from Fig. (5.1) that the shock wave keeps its identity and moves to the right at constant velocity.

Table 5.1. The invariant and the error norms for Case I over the interval [-10,10].

$p=2$ t	I	L_2	L_∞
0.0	0.0705095703	0.00000000	0.00000000
1.0	0.0688729173	0.00219512	0.00450895
2.0	0.0684210594	0.00262091	0.00462410
3.0	0.0679864368	0.00307562	0.00473738
4.0	0.0675684286	0.00354994	0.00484890
5.0	0.0671664551	0.00403901	0.00495867

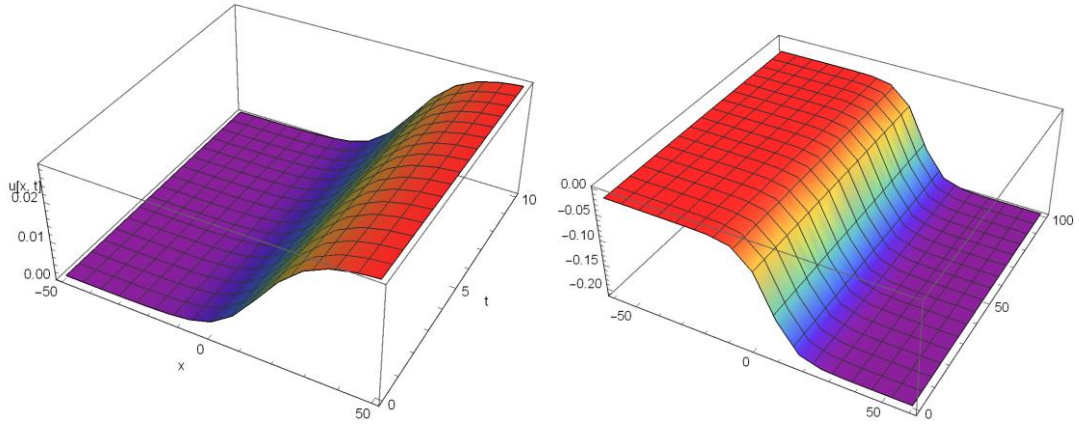

Figure 5.1. Shock wave profiles for a) p=2, γ=0.5, σ=0.1, η=7, h=0.1, a=0.3 and Δt=0.1 b) p=3, γ=0.33, σ=0.1, η=7, h=0.1, a=0.5 and Δt=0.1.

CASE 2.

As a second case, to show simulation through the interval $-10 \le x \le 10$, the parameters $\gamma = 0.33$, $\sigma = 0.1$, $\eta = 7$, $h = \Delta t = 0.1$, $a = 0.5$ are chosen for $p = 3$. Here by, it is calculated that the amplitude of shock wave has -0.116. The calculated error norms and conservation constant values are listed in Table (5.2). This table clearly shows that the error norms obtained by our method are marginally quite small. The distribution of errors at $t = 10$ are depicted in Fig. (5.2) for $p = 2$ and 3, respectively. The error aberration varies from -2×10^{-3} to 2×10^{-3} for $p = 2$ and from -4×10^{-2} and 4×10^{-2} for $p = 3$.

Table 5.2. The invariant and the error norms for Case II over the interval [-10,10].

$p=3$ / t	I	L_2	L_∞
0.0	-2.33523963	0.00000000	0.00000000
1.0	-2.32880100	0.00679857	0.00204288
2.0	-2.32274406	0.01338439	0.00406700
3.0	-2.31704365	0.01977795	0.00607621
4.0	-2.31167526	0.02599985	0.02599985
5.0	-2.30661498	0.03207079	0.01006373

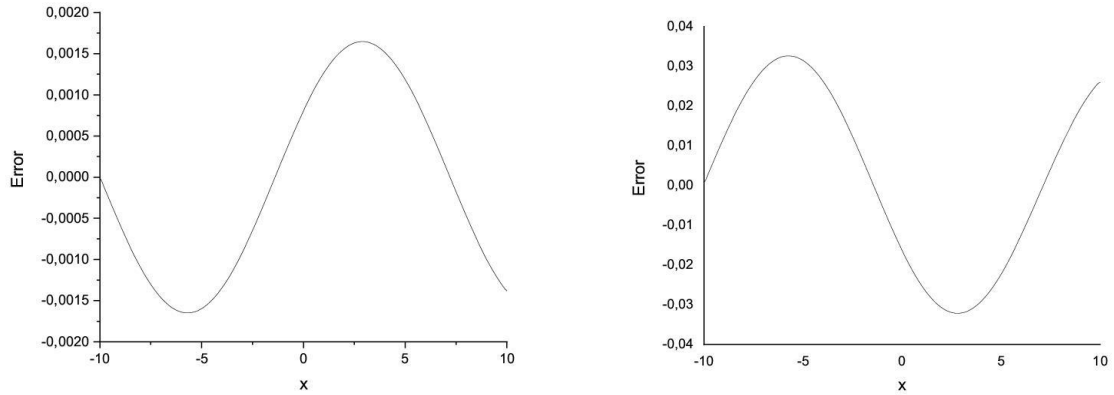

Figure 5.2. Error distributions at t=10 for the parameters a) p=2,γ=0.5, σ=0.1, η=7 and a=0.3 b) p=3, γ=0.33, σ=0.1, η=7 and a=0.5.

5.2. EVOLUTION OF WAVES

5.2.1. Gaussian initial condition

For the equation under consideration, the evolution of waves is now investigated using the Gaussian initial condition

$$U(x,0)=\exp(-x^2) \qquad (5.3)$$

and boundary condition

$$U(-10,t)=U(10,t)=0,\ t>0$$

for different values of h and Δt.

To examine the wave evolution shown below, the parameters $\sigma=0.1,\ \eta=7,\ \gamma=0.5,\ 0.33,\ p=2,\ 3,\ a=0.3,\ 0.5,\ h=\Delta t=0.1,\ 0.01$ are taken in the range $[10,10]$.

CASE 1.

The values of $\gamma=0.5,\ \sigma=0.1,\ \eta=7,\ a=0.3$ and $h=\Delta t=0.01$ are selected for $p=2$. The run of the algorithm is run to time $t=5$ to obtain the values of the invariant. The values of the the invariant quantity of motion for two different values of h and Δt are demonstrated

in Table (5.3). In this case, it can be said that the solutions reached depend on the values of h and Δt. Fig.(5.3) illustrates the development of the Gaussian initial condition into waves through the interval $x \in [-10,10]$.

CASE 2.

The parameters $\gamma = 0.33$, $\sigma = 0.1$, $\eta = 7$, $a = 0.5$ and $h = \Delta t = 0.01$ are chosen for $p = 3$. Calculations are realized from $t = 0$ to $t = 5$. The values of the conserved invariant of motion are given in Table (5.3) for different values of time and space steps. It can be said from the Table (5.3) that the invariant is very close to each other as time increases. Therefore, it can said that our method is sensibly conservative. The evolution of a train of waves with Gaussian initial condition is plotted in Fig. (5.3) for $p = 3$.

Table 5.3. Invariant and error norms for Gaussian initial condition

t	$p=2$		$p=3$	
	$h=\Delta t=0.1$	$h=\Delta t=0.01$	$h=\Delta t=0.1$	$h=\Delta t=0.01$
	I	I	I	I
0.0	1.7724537283	1.7724549574	1.7724537283	1.7724549574
1.0	1.8025375281	1.8025515254	1.8022592747	1.8024322019
2.0	1.8315838133	1.8316063645	1.8310659550	1.8314024588
3.0	1.8590051123	1.8590509111	1.8586491384	1.8591428539
4.0	1.8842829125	1.8843701948	1.8848031508	1.8854496139
5.0	1.9065605329	1.9071105522	1.9093419082	1.9101386384

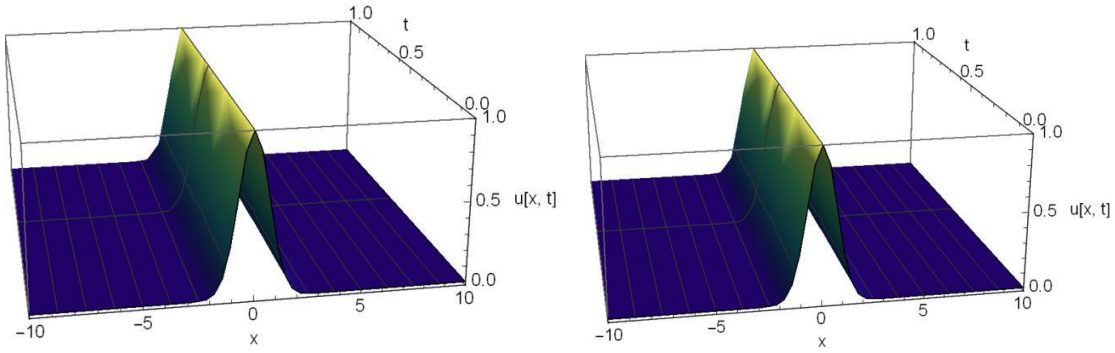

Figure 5.3. Generated waves profiles with a) p=2, γ=0.5, σ=0.1, η=7 and a=0.3 b) p=3, γ=0.33, σ=0.1, η=7 and a=0.5 with various values of h and Δt.

5.2.2 Undular bore initial condition

In this part, evolution of a train of waves of the generalised Oskolkov equation is processed using the undular bore initial condition and boundary condition

$$U(x,0) = \frac{1}{2}U_0\left[1-\tanh\left(\frac{|x|-x_0}{d}\right)\right], \qquad (5.4)$$
$$U(-60,t) = U(60,t) = 0, \quad t > 0$$

cause to produce a train of solitons for generalised Oskolkov equation. If the transition between the depths has only a slight slope, a bore is formed when a deeper stream of water flows into the still water area [36]. The changing in amplitude is centered on $x = x_0$ and the steepness of the change is measured by d. The values of d is inversely proportional to the steepness [37]. The parameters are choosen as $\sigma = 0.1,\ \eta = 7,\ U_0 = 0.25,\ x_0 = 25$ and $d = 5$ in Eq. (5.4).

CASE 1.

In the first case, the parameters $\gamma = 0.5,\ \sigma = 0.1,\ \eta = 7,\ a = 0.3$ and $h = \Delta t = 0.1,\ 0.02$ are taken for $p = 2$. The numerical study was calculated up to $t = 5$. Variation of the conserved quantity position is reported in Table (5.4). Fig.(5.4) indicates the simulation of waves at $t = 5$. It can be clearly said that the undulation bore maintains the steady state during operation, which can be observed in Fig.(5.4) from $t = 0$ to $t = 100$.

CASE 2.

In this simulation, for comparison with earlier case, the parameters $\gamma = 0.33,\ \sigma = 0.1,\ \eta = 7,\ a = 0.5$ and $h = \Delta t = 0.1,\ 0.02$ are chosen for $p = 3$. The run of the algorithm is continued up to time $t = 5$ over the problem region $-60 \le x \le 60$. The values of the invariant obtained from present method are given in Table(5.4). The evolution of the waves is samplied in Fig. (5.4) from $t = 0$ to $t = 100$.

Table 5.4. Invariant and error norms for Undular bore initial condition

	$p = 2$		$p = 3$	
t	$h = \Delta t = 0.1$	$h = \Delta t = 0.02$	$h = \Delta t = 0.1$	$h = \Delta t = 0.02$
	I	I	I	I
0.0	12.5000275676	12.4998649440	12.5000275676	12.4998649440
1.0	12.4968960273	12.4967407712	12.4986970475	12.4985477436
2.0	12.4870227201	12.4869144654	12.4947142014	12.4945965316
3.0	12.4687265050	12.4687427378	12.4873844225	12.4873318673
4.0	12.4396450182	12.4399136353	12.4757710379	12.4758377388
5.0	12.3966116239	12.3973296490	12.4586439575	12.4589122926

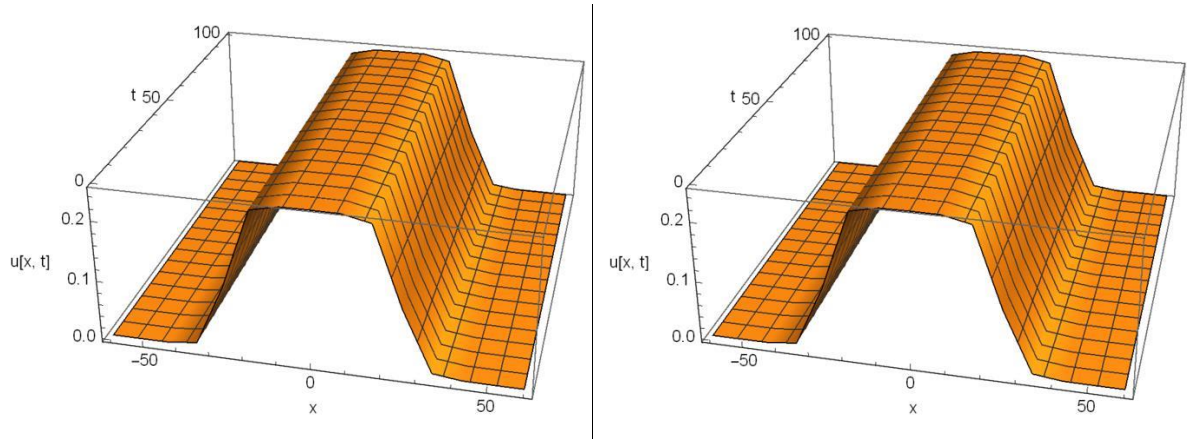

Figure 5.4. Generated waves with a) γ=0.5, σ=0.1, η=7 and a=0.3 b) γ=0.33, σ=0.1, η=7 and a=0.5 with various values of h and Δt.

6. CONCLUSIONS

In this research, a collocation method based on quintic B-splines has been constructed for obtaining the numerical solutions of the generalised Oskolkov equation. Stability analysis has been done and the suggested method has been shown to be unconditionally stable. The method is implemented through shock wave and evolution of waves with Gaussian and undular bore initial condition; for shock wave L_2 and L_∞ error norms and for the Gaussian and undular bore initial condition the invariant quantity I have been calculated. Furthermore the theoretical bound of the error in such a full discrete approximation has been demonstrated. From the calculated results it is obviously clear that the error norms are quite small, and the invariant is almost constant in all computers run. Finally, it could be recommended that the method can be used to solve a wide range of different partial differential equations.

REFERENCES

[1] Hosseini, K., Bejarbaneh, E.Y., Bekir, A., Kaplan, M., *Optical and Quantum Electronics*, **49**(7), 1, 2017.
[2] Karakoc, S.B.G., Saha, A., Sucu, D., *Chinese Journal of Physics*, **68**, 605, 2020.
[3] Roshid, M., Bashar, H., *Mathematical Modelling of Engineering Problems*, **6**(3), 460, 2019.
[4] Yaşar, E., Yildirim, Y., Adem, A.R., *Optik*, **158**, 1, 2018.
[5] Roshid, H.O., Roshid, M.M., Rahman, N., Pervin, M.R., *Propulsion and Power Research*, **6(**1), 49, 2017.
[6] Roshid, H.O., Hoque, M.F., Akbar, M.A., *Springer Plus*, **3**, 122, 2014.
[7] Feng, L.L., Zhang, T.T., *Applied Mathematics Letters*, **78**, 133, 2018.
[8] Xu, S.W., He, J.S., *Journal of Mathematical Physics*, **53**, 063507, 2012.
[9] Dai, C.Q., Zhang, J.F., *Chaos, Solitons & Fractals*, **27**, 1042, 2006.
[10] Tian, S.F., Zhang, T.T., *Proceedings of the American Mathematical Society*, **146**, 1713, 2018.
[11] Biswas, A., Mirzazadeh, M., Eslami, M., Zhou, Q., Bhrawy, A., Belic, M., *Optik*, **127**(18), 7250, 2016.
[12] Yildirim, A., Pinar, Z., *Computers & Mathematics with Applications*, **60**(7), 1873, 2010.
[13] Zhao, Y.M., *Journal of Applied Mathematics*, **2014**, 848069, 2014.
[14] Triki, H., Ak, T., Ekici, M., Sonmezoglu, A., Mirzazade, M., Kara, A., Aydemir, T., *Nonlinear Dynamics*, **89**(2), 501, 2017.
[15] Alquran, M., *Journal of Mathematical and Computational Science*, **2**(1), 15, 2012.
[16] Khan, K., Akbar, M.A., Alam, M.N., *Journal of the Egyptian Mathematical Society*, **21**(3), 233, 2013.
[17] Sviridyuk, G.A., Shipilov, A.S., *Differential Equations*, **46**(5), 742, 2010.
[18] Akcagil, S., Aydemir, T., Gozukizil, O.F., *New Trends in Mathematical Sciences*, **4**(4), 51, 2016.
[19] Roshid, M.M., Roshid, H.O., *Heliyon*, **4**, e00756, 2018.
[20] Gozukizil, O.F., Akcagil, S., *Advances in Difference Equations*, **143**, 2, 2013.
[21] Ak, T., Aydemir, T., Saha, A., Kara, A., *Pramana – Journal of Physics*, **90**(6), 78, 2018.
[22] Kondyukov, A.O., Sukacheva T.G., *Computational Mathematics and Mathematical Physics*, **55**(5), 823, 2015.
[23] Prenter, P.M., *Splines and variational methods*, Dover Publications, Mineola, 2008.

[24] Rubin, S.G., Graves, R.A.Jr., *Computers & Fluids*, **3**(1), 1, 1975.
[25] Karaagac, B., Ucar, Y., Esen, A., *Filomat*, **32**(16), 5573, 2018.
[26] Karakoc, S.B.G., Omrani, K., Sucu, D., *Applied Numerical Mathematics*, **162**, 249, 2021.
[27] Bochev, P.B., Gunzburger M.D., The Agmon–Douglis–Nirenberg Setting for Least-Squares Finite Element Methods. In Gunzburger M.D., Bochev, P.B. (Eds.), *Least-Squares Finite Element Methods*, part of book series: Applied Mathematical Sciences, Vol. 166, Springer-Verlag, New York, 2009.
[28] Suli, E., Mayers, D.F., *An introduction to numerical analysis*, Cambridge University Press, Cambridge, 2003.
[29] Thomee, V., *Galerkin Finite Element Methods for Parabolic Problems*, 2nd Ed., Springer-Verlag, New York, 2006.
[30] Bhowmik, S.K., Belbakib, R., Boulmezaoudc, T.Z., Mziou, S., *Computers & Mathematics with Applications*, **67**(10), 2027, 2014.
[31] Ak, T., Dhawan, S., Karakoc, S.B.G., Bhowmik, S.K., Raslan, K.R., *Mathematical Modelling and Analysis*, **22**(3), 373, 2017.
[32] Gomez, H., Lorenzis, L.D., *Computer Methods in Applied Mechanics and Engineering*, **309**, 152, 2016.
[33] Bhowmik, S.K., *Journal of Mathematical Analysis and Applications*, **420**(2), 1069, 2014.
[34] Dhawan, S., Bhowmik, S.K., Kumar, S., *Applied Mathematics and Computation*, **261**, 128, 2015.
[35] Dhawan, S., Ak, T., Apaydin, G., *International Journal of Modern Physics* C, **30**(11), 1, 2019.
[36] Ak, T., Mohammed, S.O., Kara, A., *Journal of Applied Analysis and Computation*, **10**(5), 2145, 2020.